Journal of
Materials Chemistry A

RSCPublishing

PAPER

View Article Online
View Journal | View Issue

Published on 12 November 2012. Downloaded by New York University on 08/10/2014 11:56:32.

Cite this: *J. Mater. Chem. A*, 2013, **1**, 1465

Polymer electrolyte membranes based on poly(arylene ether)s with penta-sulfonated pendent groups

Jinhui Pang,* Kunzhi Shen, Dianfu Ren, Sinan Feng, Yang Wang and Zhenhua Jiang

Received 18th September 2012
Accepted 9th November 2012

DOI: 10.1039/c2ta00363e

www.rsc.org/MaterialsA

The preparation and characterization of new polymeric ionomers based on a fully aromatic poly(arylene ether) backbone with locally pentasulfonated pendent groups for applications as proton exchange membranes is reported. The high molecular weight sulfonated polymers were obtained by the polycondensation of new (2,6-difluorophenyl) (4-(1,2,3,4,5-pentaphenylbenzene)phenyl)methanone, 4,4′-difluorodiphenyl methanone, and 4,4′-dihydroxydiphenylsulfone, followed by sulfonation using sulfuric acid in high yields. The polymers produced tough, flexible, and transparent membranes by solvent casting. Membranes with ion exchange capacities between 0.8 and 1.7 mEq g^{-1} showed high proton conductivities and low methanol permeabilities. Compared to Nafion 117, these sulfonated membranes exhibited better microphase separation morphologies. The fully humidified membranes also exhibited considerably good mechanical properties, with tensile strengths from 35 to 45 MPa and elongations at break from 23 to 49%. This investigation demonstrates a controllable high density sulfonated side group of a poly(arylene ether sulfone) membrane with tunable and balanced properties, which is promising for proton exchange membrane fuel cell technology.

Introduction

Polymer electrolyte membrane fuel cells (PEMFCs) are under consideration as future power sources for transport, stationary and portable applications.[1–3] One of the key materials in a PEMFC is a proton exchange membrane (PEM), which allows for proton transport from the anode to the cathode. The current state-of-the-art PEM materials are perfluorinated polymers such as Nafion or Flemion because of their good physical and chemical stabilities along with their high proton conductivities over a wide range of relative humidities at moderate operation temperatures. However, these membranes still have a number of drawbacks especially for large-scale applications, such as high cost, high methanol permeability, and poor performance at temperatures above 80 °C, which calls for the development of new membrane materials.[4,5]

Aromatic hydrocarbon polymers are alternative PEM materials, and a number of sulfonated aromatic polymers such as poly(ether ether ketone)s,[6–10] polyimides,[11,12] and polybenzimidazole have been developed as suitable candidates.[13] Generally, membranes based on these polymers require high ion exchange capacities (IECs) to achieve proton conductivities comparable to those of perfluorinated polymers. Although a high IEC value results in a high conductivity for a polymer, excessive water uptake may result in exorbitant dimensional change as well as decreased mechanical strength of the film.[14–16] As a strategy to improve the proton conductivity and mechanical properties, sulfonated side chain and sulfonated multiblock copolymers have been extensively studied.[17–20] The technique with sulfonated side chain PEMs is to design a polymer architecture that distinctly separates the hydrophilic sulfonic acid groups from the hydrophobic polymer main chain by locating the sulfonic acid groups on flexible side chains, which may induce improved nanophase separation between the hydrophilic and hydrophobic domains. For example, Guiver and co-workers reported PEMs prepared by attaching flexible pendent sulfonated aromatic side chains to poly(arylene ether sulfone), which showed a superior proton conductivity of 147 mS cm^{-1} at 80 °C with a slightly higher water content than Nafion.[21] Our group also reported PEMs based on poly(arylene ether) with aromatic or aliphatic sulfonated side chains,[22–24] which exhibited high proton conductivities and excellent dimensional stabilities. Another approach to induce nanophase separation is through sulfonated multiblock copolymer architecture, whereby sulfonic acid groups are concentrated in blocks along the polymer chain. McGrath *et al.*[25] prepared multiblock sulfonated poly(arylene ether)s with promising morphological structures by two-step polycondensation. The fuel cell performance of a single cell using this multiblock copolymer at 40% RH (relative humidity) was comparable to that of Nafion, and it performed much better than the alternating and random polymers. More recently, random copolymers designed with densely localized concentrations of sulfonated units in the

---

Alan G. MacDiarmid Institute, Department of Chemistry, Jilin University, No. 2699 Qianjin street, Changchun, P.R. China. E-mail: pangjinhui@jlu.edu.cn; Fax: +86 431 85168199; Tel: +86 431 85168199

This journal is © The Royal Society of Chemistry 2013

Published on 12 November 2012. Downloaded by New York University on 08/10/2014 11:56:32.

main chains have attracted considerable attention because of the high contrast in polarity between the hydrophilic and hydrophobic units; this promotes the formation of hydrophilic–hydrophobic phase-separated structures. It has been found that the morphological structures of the copolymers were comparable to that of Nafion 117, which explains their high proton conductivities.[26,27] On the other hand, Hay *et al.* reported poly(arylene ether)s with high density sulfonated endcaps, in order to enhance the difference between the hydrophilic and hydrophobic units.[28,29] Their membranes showed significantly phase-separated morphologies. However, their structures were limited in the number of sulfonated units because the number of terminated groups was restricted. Furthermore, hydrophilic units at the periphery increase the water solubility of polymers, which prevents an increase in the IEC values.

In this paper, we attempt to attach high density sulfonated groups into the side chains of poly(arylene ether) and prepare poly(arylene ether) containing higher density pentasulfonated side chains. We investigate the relationship between the structure, morphology and properties.

Materials

2,6-Difluorobenzoyl chloride, phenylacetylene, tetraphenylcyclopentadienone, PPh_3, CuI, and $PdCl_2(PPh_3)_2$ were purchased from Sigma-Aldrich Ltd. Sulfolane, bromobenzene, TEA (triethylamine), DMAc (dimethylacetamide), and toluene were purchased from Shanghai Chemical Reagent Co. Ltd. 4,4′-Dihydroxydiphenylsulfone, 4,4′-difluorodiphenyl methanone, and K_2CO_3 were purchased from Sinopharm Chemical Reagent Beijing Co. Ltd. Other commercially available materials and solvents were used without further purification.

Synthesis of monomer

(4-BROMOPHENYL)(2,6-DIFLUOROPHENYL)METHANONE (**1**). A 250 mL three-neck flask equipped with a mechanical stirrer, a dropping funnel, and a nitrogen inlet was charged with 100 mL of bromobenzene. The solution was cooled to 0 °C, and anhydrous $AlCl_3$ (14.6 g, 0.11 mol) was added in several portions. After the solution had been stirred for 10 min, 2,6-difluorobenzoyl chloride (17.6 g, 0.1 mol) was added dropwise over 10 min. Then the temperature was raised to 90 °C and maintained there for 8 h. The mixture solution was poured into 100 mL of 1 M hydrochloric acid ice-water solution after the reaction solution had cooled to room temperature. The organic phase was separated and washed with 10% NaOH (1 × 100 mL) and H_2O (4 × 100 mL). The solution was dried with anhydrous $MgSO_4$, and the excess bromobenzene was evaporated under vacuum. After being recrystallized in petroleum (60–90 °C) and dried, 26.7 g of white crystals was obtained. Yield: 90%. Mp (melting point): 86 °C. δ_H (500 MHz; $CDCl_3$; Me_4Si): 6.98–7.05 (2H, m, FPh), 7.42–7.52 (1H, m, FPh), 7.61–7.65 (2H, m, BrPh), 7.71–7.75 (2H, m, COPh). Mass spectrum: *m*/*z* 299 (H^+), 336.3 (K^+).

(2,6-DIFLUOROPHENYL)(4-(PHENYLETHYNYL)PHENYL)METHANONE (**2**). **1** (14.85 g, 0.05 mol) and 150 mL of triethylamine were added to a 250 mL, three-necked, round-bottom flask equipped with a mechanical stirrer, a nitrogen inlet/outlet, and a reflux condenser. Triphenylphosphine (PPh_3; 0.1 g), $PdCl_2(PPh_3)_2$ (0.05 g), and cuprous iodide (CuI; 0.05 g) were added and washed down with 50 mL of triethylamine. The mixture was slowly heated to 60 °C in an oil bath, and phenylacetylene (5.5 mL, 0.05 mol) was added with another 40 mL of triethylamine. The reaction temperature was raised and maintained at 80 °C for 4 h. After the mixture had cooled to room temperature, the reaction subsequently proceeded for about 16 h. The mixture was filtered to provide a white, solid filter cake, which was washed with distilled water twice to remove the inorganic salts that formed, and the crude product was recrystallized from acetone. A dried white crystal (11.9 g) was obtained in a yield of 75.1%. Mp: 130 °C. δ_H (500 MHz; $CDCl_3$; Me_4Si): 6.99–7.05 (2H, m, FPh), 7.36–7.39 (3H, m, Ph), 7.41–7.53 (1H, m, FPh), 7.54–7.58 (2H, m, C≡CPh), 7.61–7.65 (2H, m, C≡CPh), 7.84–7.87 (2H, m, COPh). Mass spectrum: *m*/*z* 317.5.

(2,6-DIFLUOROPHENYL) (4-(1,2,3,4,5-PENTAPHENYLBENZENE) PHENYL)METHANONE(**3**). To a three neck round-bottomed flask equipped with a mechanical stirrer and an argon in–out channel, compound **2** (3.18 g, 10 mmol), tetraphenylcyclopentadienone (3.84 g, 10 mmol), and sulfolane (5 mL) were added and heated at 250 °C for 3 h under argon. After cooling the mixture was poured into methanol and the precipitate was purified by recrystallization from toluene to give 6.1 g of **3** as a light yellow powder in a yield of 90%. Mass spectrum: *m*/*z* 675.4, 698.6 (Na^+), 714.9 (K^+).

Synthesis and sulfonation of the poly(arylene ether) copolymer

SYNTHESIS OF NONSULFONATED POLY(ARYLENE ETHER)S (**P-*x***). A typical polycondensation procedure was conducted as follows (Scheme 2): to a round-bottomed flask equipped with a Dean–Stark trap, 4,4′-difluorodiphenyl methanone (0.9819 g, 4.5 mmol), **3** (0.3374 g, 0.5 mmol), 4,4′-dihydroxydiphenylsulfone (1.2514 g, 5.0 mmol), and K_2CO_3 (0.759 g, 5.05 mmol) were added. Then, sulfolane (8 mL) and toluene (3 mL) were added into the flask under argon. The reaction mixture was stirred at 140 °C for 3 h. After the removal of toluene, the reaction temperature was increased to 220 °C, and the reaction was continued for 6 h. After cooling to room temperature, the mixture was poured into deionized water. The resulting fiber was filtered and washed with hot deionized water and hot ethanol. The polymer was dried under vacuum at 120 °C for 12 h to give pure nonsulfonated poly(arylene ether) **P-10** ($x = 10$). The yield was 98%.

SYNTHESIS OF THE SULFONATED POLY(ARYLENE ETHER)S (**SP-*x***). **P-*x*** (1 g) and 10 mL H_2SO_4 (95–98%) were put into a 100 mL single neck round-bottomed flask. The reaction mixture was stirred at room temperature for 12 h. Then the yellow mixture solution was poured into ice-water, and a flexible polymer fiber was obtained. The fiber was filtered and washed with hot deionized water and hot ethanol. The polymer was dried under vacuum at 120 °C for 12 h to give pure sulfonated poly(arylene ether)s **SP-*x***. The yield remained above 97%.

This journal is © The Royal Society of Chemistry 2013

Published on 12 November 2012. Downloaded by New York University on 08/10/2014 11:56:32.

Analysis and measurements of the copolymers

The viscosities of the obtained copolymers were determined by using an Ubbelohde viscometer in a thermostatic container with a polymer concentration of 0.5 g dL^{-1} in DMAc at 25 °C. FT-IR spectra (film) were measured on a Nicolet Impact 410 Fourier-transform infrared spectrometer. ^{1}H NMR experiments were carried out on a Bruker 510 spectrometer (^{1}H, 500 MHz) using DMSO-d$_6$ and CDCl$_3$ as solvents.

Film formation and proton exchange

SP-*x* copolymer (1.0 g) was dissolved in DMAc (10 mL) overnight. Afterwards, the solution was filtered with a fine glass fritted filter funnel and cast directly onto clean glass plates. After being carefully dried at 60 °C for 10 h and vacuum-dried at 120 °C for 24 h, tough and flexible films of **SP-*x*** were obtained. The membranes were transformed to the acid forms by proton exchange in 1 M H_2SO_4 for 24 h at room temperature. Then, the membranes were soaked and washed thoroughly with deionized water. The thicknesses of the membranes were in the range of 70–90 μm.

Thermal properties of the membranes

Differential scanning calorimetry (DSC) measurements were performed on a Mettler Toledo DSC821e instrument at a heating rate of 10 °C min^{-1} from 50 to 300 °C under nitrogen. Thermogravimetric analysis (TGA) on a Perkin Elmer Pyris 1 thermal analyzer system was employed to assess the thermal stability of the membranes. Before the analysis, the membranes were dried and kept in the TGA furnace at 120 °C under air for 30 min to remove water. The samples were evaluated over a temperature range of 100–800 °C at a heating rate of 10 °C min^{-1} under N_2.

Ion exchange capacity

The ion exchange capacity (IEC) values of the membranes were determined by acid–base titration. The dried membrane was weighed and immersed in 1.0 M H_2SO_4 solution for 24 h to protonize the sulfonic acid groups and was then washed thoroughly with deionized water until the pH was neutral. The membrane was then immersed in a 2.0 M solution of NaCl for 12 h to replace the protons of the sulfonic acid groups with sodium ions. The solutions were titrated using 0.02 M NaOH solution, with phenolphthalein as the indicator. The IEC values were calculated from the titration results as the ratio of the amount of NaOH consumed (mmol) to the weight of the dried membrane samples (g).

Water uptake and swelling ratio measurements

The membranes were soaked in deionized water to reach equilibrium at the desired temperature. The membranes were then dried at 120 °C for 24 h. The weights and lengths of the dry and wet membranes were measured. The water uptake content was calculated by

$$\text{Water uptake} = \frac{W_{\text{wet}} - W_{\text{dry}}}{W_{\text{dry}}} \times 100\%$$

where W_{dry} and W_{wet} are the weights of the dried and wet samples, respectively. The swelling ratio was calculated from the change of the film length by

$$\text{Swelling ratio} = \frac{L_{\text{wet}} - L_{\text{dry}}}{L_{\text{dry}}} \times 100\%$$

where L_{wet} and L_{dry} are the lengths of the wet and dry membranes, respectively.

Oxidative and hydrolytic stability

A small piece of the membrane sample was soaked in Fenton's reagent (3% H_2O_2 aqueous solution containing 2 ppm $FeSO_4$) for 1 h at 80 °C. The oxidative stability was evaluated from the change in weight and appearance of the test sample.

Proton conductivity and methanol permeability

Fully hydrated membranes (4 cm × 1 cm) were measured by a four-electrode AC impedance method from 0.1 Hz to 100 kHz with 10 mV AC perturbation and 0.0 V DC rest voltage using a Princeton Applied Research Model 273A Potentiostat (Model 5210 frequency response detector, EG&G PARC, Princeton, NJ). The measurements were carried out with the cells immersed in the constant-temperature water, and the proton conductivity was determined by the equation:

$$\sigma = \frac{L}{RA}$$

where σ is the proton conductivity, L is the distance between the electrodes used to measure the potential ($L = 1$ cm), R is the membrane resistance, and A is the membrane area.

A stainless steel diffusion cell was used to measure the methanol permeability as described in the literature.[32] The cell consisted of two reservoirs that were separated by a membrane. A 10 M methanol solution and deionized water were placed on each side.

Magnetic stirrers were used in each compartment to ensure uniformity. The concentration of the methanol in the water reservoir was determined by using a SHIMADZU GC-8A chromatograph. The methanol permeability was calculated as follows:

$$C_{\text{B}}(t) = \frac{A}{V_{\text{B}}}\frac{\text{DK}}{L}C_{\text{A}}(t - t_0)$$

where A (in cm^2), L (in cm), and V_{B} (in mL) are the effective area, the thickness of the membrane, and the volume of the permeated reservoirs, respectively. C_{A} and C_{B} (in mol L^{-1}) are the methanol concentration in the feed and in the permeate, respectively. t and t_0 (in s) represents time and the time lag, respectively. DK (in cm^2 s^{-1}) denotes the methanol permeability.

The methanol uptake and the swelling ratio in high concentration methanol solution (10 mol L^{-1}) were measured in the same way as they were measured in water, which is described above.

Published on 12 November 2012. Downloaded by New York University on 08/10/2014 11:56:32.

Morphology

SAXS measurements were carried out on membranes ion-exchanged to the Pb^{2+} form by immersion in a 1 wt% aqueous solution of lead acetate. The scattering experiments were performed on a SAXSess camera equipped with a CCD detector. CuKα radiation with a wave length (λ) of 0.1542 nm was generated by a Rigaku D/max-2550 X-ray generator operating at 50 kV and 200 mA. Dry membranes were analyzed in a solid sample holder at 25 °C. The wave vector (q) was calculated according to:

$$q = 4\pi\lambda^{-1}\sin\theta$$

where 2θ is the scattering angle. The characteristic separation length (d), *i.e.* the Bragg spacing, was calculated as:

$$d = 2\pi q^{-1}$$

Mechanical properties

The mechanical properties of the dry/wet membranes were measured at room temperature on a SHIMADIU AG-I 1KN at a strain rate of 2 mm min^{-1}. The size of the samples was 20 mm × 4 mm. The membranes were dried at 120 °C under vacuum for 12 h. The samples in the wet state were obtained by immersing them in water for 12 h.

Results and discussion

Synthesis of monomer

As a new difluoride monomer having five sulfonation positions, (**3**) was designed and prepared as shown in Scheme 1. Monomer **3** was prepared by a three-stage synthetic procedure starting with the Friedel–Crafts reaction of 2,6-difluorobenzoyl chloride and bromobenzene to give compound **1**. Then compound **2** was obtained by a palladium-catalyzed Sonogashira coupling reaction of compound **1** and phenylacetylene.[30] Finally, as described similarly in the literature,[28,31] the multi-phenyl compound **3** was synthesized through a Diels-Alder reaction. The structures of these compounds were confirmed by FT-IR, LC-MS and ^{1}H NMR spectroscopy. As shown in Fig. 1, the structure of the monomer **3** was confirmed using ^{1}H NMR spectroscopy. The signals at 7.3–7.4 ppm were assigned to the protons in the benzophenone structure of monomer **3**, while those at 6.8–7.0 ppm were assigned to the electron-rich phenyl groups.

Synthesis of poly(arylene ether) copolymer

A series of poly(arylene ether) polymers with pendent penta-sulfonation sites were successfully synthesized *via* a standard aromatic nucleophilic substitution reaction of monomer **3** with 4,4′-difluorobenzophenone and 4,4′-dihydroxydiphenylsulfone, and were named **P-*x*** (as shown in Table 1 and Scheme 2, ***x*** is the ratio of monomer **3** in the copolymer). A sulfone and carbonyl-rich main chain was selected because of its high adaptability for PEM application. The content of the difluoride monomer **3** in the copolymerization procedure can control the IEC after sulfonation. All the polymers (**P-*x***) were soluble in chloroform, THF and polar aprotic solvents. The structure of the polymers **P-*x*** were confirmed by ^{1}H NMR spectroscopy. The ^{1}H NMR spectrum of the polymer **P-20** is shown in Fig. 2. Several specific protons were clearly assigned, and the expected copolymer structure was confirmed. The integral ratio of the peaks from 6.5 to 7.1 ppm which were assigned to the protons in the monomer **3** moieties and all proton peaks was calculated to determine the composition of the polymer. The calculated result (x = 20) matched well with its initial composition.

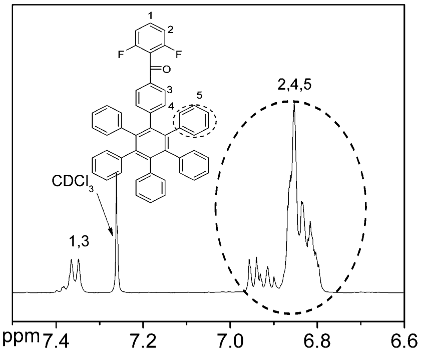

Fig. 1 ^{1}H NMR spectrum of the monomer **3**.

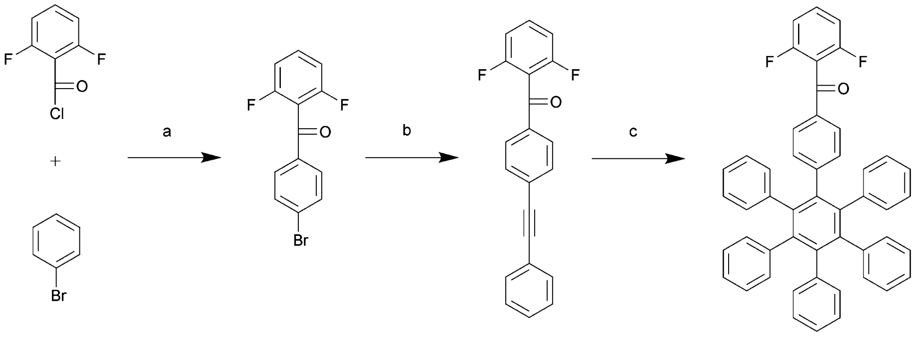

1

2

3

Scheme 1 Synthesis of the difluoride monomer. a: $AlCl_3$, 100 °C, 6 h. b: Phenylacetylene, TEA, $PdCl_2(PPh_3)_2$, PPh_3, CuI. c: Tetraphenylcyclopentadienone, 250 °C, 3 h.

Published on 12 November 2012. Downloaded by New York University on 08/10/2014 11:56:32.

Table 1 Intrinsic viscosities, ion exchange capacities (IECs), and thermal properties of sulfonated polymers **SP-*x***

Polymer	x	IEC[a] (mEq g^{-1})	IEC[b] (mEq g^{-1})	$[\eta]$ (dL g^{-1})	T_g (°C)	T_d[c] (°C)	T_d[d] (°C)
SP-20	20	1.67	1.53	1.20	222	238	360
SP-18	18	1.55	1.46	1.33	214	239	365
SP-16	16	1.42	1.35	1.08	210	240	372
SP-14	14	1.28	1.20	0.91	205	242	378
SP-12	12	1.13	1.01	0.87	203	246	386
SP-10	10	0.97	0.92	0.77	200	248	393
SP-8	8	0.80	0.80	0.61	199	251	404

[a] Theoretical value. [b] Calculated by titration. [c] Onset weight loss temperature. [d] 5% weight loss temperature.

Sulfonation of the copolymers

The copolymers were sulfonated using sulfuric acid (95–98%) at room temperature. We chose 4,4′-difluorobenzophenone and 4,4′-dihydroxydiphenylsulfone as the other two monomers in the copolymerization because of their strongly electron-withdrawing groups, ketone or sulfone. According to literature

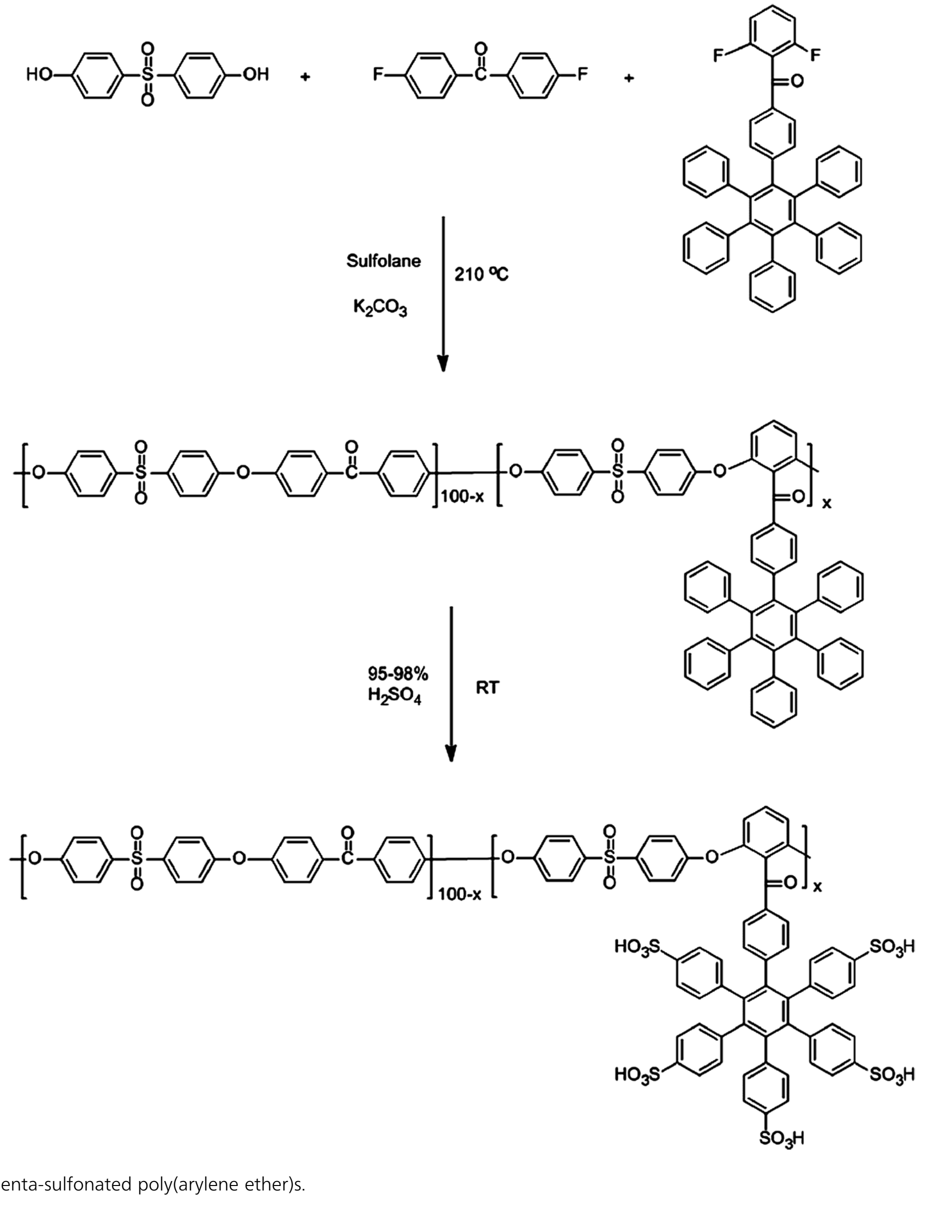

Scheme 2 Synthesis of penta-sulfonated poly(arylene ether)s.

Published on 12 November 2012. Downloaded by New York University on 08/10/2014 11:56:32.

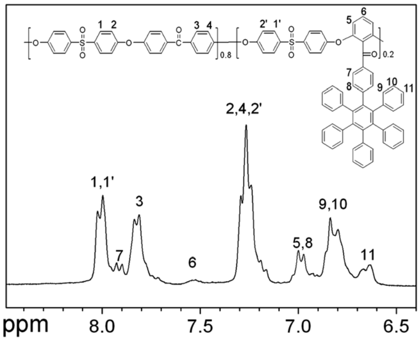

Fig. 2 ^{1}H NMR spectrum of the poly(arylene ether) copolymer (**P-20**).

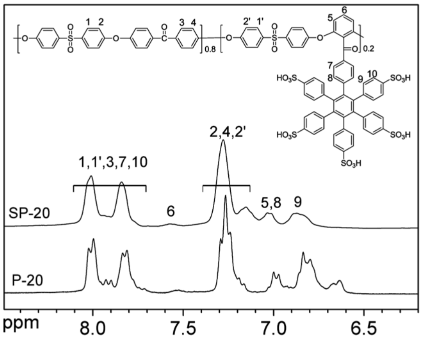

Fig. 4 ^{1}H NMR spectrum of the sulfonated poly(arylene ether) copolymer (**SP-20**).

reports,[28,33] polymer main chains containing diphenylsulfone and benzophenone moieties have excellent stabilities even under the harsh sulfonation conditions so that neither sulfonation nor chain cleavage occurs. Therefore, the sulfonated reaction occurred on the electron-rich aromatic pendant phenyls in the side chain. In order to achieve complete sulfonation to **P-*x***, an excess amount of sulfonic acid was used. After sulfonation the reaction mixture was put into deionized water to remove excess sulfuric acid, and the product was dried to give **SP-*x***. The **SP-*x*** was readily soluble in polar aprotic solvents such as DMF, DMAc, DMSO and NMP. Tough, flexible and transparent membranes of **SP-*x*** were obtained by a solution casting method. The structures of **SP-*x*** were confirmed by FT-IR and ^{1}H NMR spectroscopy. As shown in Fig. 3, the characteristic IR absorption of the sulfonic acid group ($\nu_{S=O}$) and diphenylcarbonyl ($\nu_{C=O}$) were observed at 1038 and 1658 cm^{-1}, respectively. These results confirmed the successful introduction of the sulfonic acid groups onto the polymer side chains. Fig. 4 shows the ^{1}H NMR spectra of **P-20** and **SP-20**. In comparing the spectra before and after sulfonation, the peak (H_{11}) at 6.65 ppm has disappeared completely after sulfonation, which indicates that complete sulfonation occurred on each pendent phenyl ring of the **SP-20**.

The elementary characterization data for **SP-*x*** are summarized in Table 1. Experimental ion exchange capacities (IECs) of **SP-*x*** were determined by titration of the membranes in acid form with sodium hydroxide. The results show IEC values compared to the theoretical value which is calculated by considering a proton of each sulfonic acid group in the repeat unit (Table 1). The viscosity values of the resulting **SP-*x*** were in the range 0.6–1.3 dL g^{-1}, indicating their high molecular weights.

Thermal properties

The thermal stabilities of **P-*x*** and **SP-*x*** were evaluated using a TGA instrument under a nitrogen atmosphere. The **P-*x*** exhibited high thermal degradation temperatures. The onset weight loss temperature is higher than 450 °C and the 5% weight loss temperatures are above 500 °C, indicating their high thermal stabilities. Compared to **P-*x***, the **SP-*x*** have lower onset weight loss temperatures (Table 1 and Fig. 5). However it is higher than 240 °C, meeting a requirement of PEMFCs. All the **SP-*x*** exhibited a two-step degradation profile. As shown in Fig. 5, the **SP-8** and **SP-20** degradation processes were observed clearly. The first weight loss at about 250 °C was attributed to the degradation of the sulfonic acid groups, while the second weight loss peak at about 400 °C was due to the degradation of the main chains of the sulfonated polymers. The T_g (glass transition temperature) values of the **P-*x*** were over 190 °C, and those of the **SP-*x*** were observed before degradation occurred. The T_g values of the sulfonated copolymers are much higher than those of the non-sulfonated ones, since chain rigidity is increased through hydrogen bonding interactions of the sulfonic acid groups.

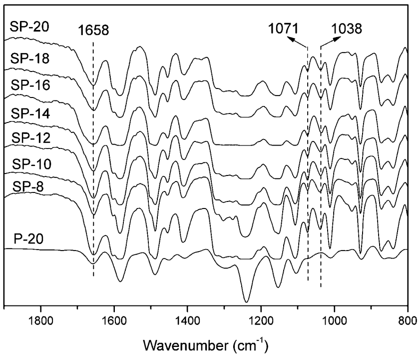

Fig. 3 FT-IR of the copolymers.

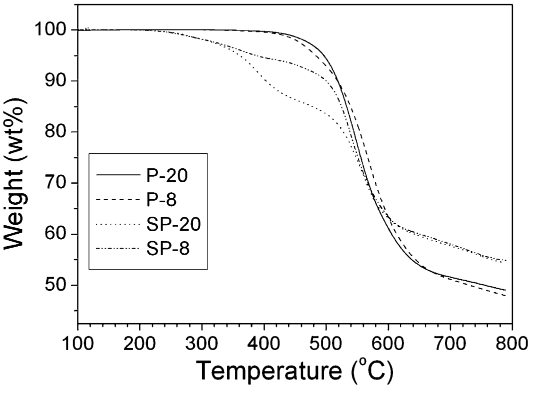

Fig. 5 TGA curves of the copolymers.

This journal is © The Royal Society of Chemistry 2013

Published on 12 November 2012. Downloaded by New York University on 08/10/2014 11:56:32.

Water uptake, swelling ratio and oxidative stability

Water uptake is very closely related to the proton conductivities and the mechanical properties of PEM materials. Appropriate water absorption helps form connected hydrophilic channels which serve as a proton transport medium. However, excess water in the polymer may destroy the hydrophobic phase leading to a loss of mechanical properties, and may even result in the polymer film being soluble in water. Several methods have been probed to study the morphology effects on the water absorption behavior and conductivity of copolymer, to investigate the relationship between the polymer structure and proton conductivity and dimension stability. We focus on the introduction of high density sulfonic acid on the end of the side chains of the poly(arylene ether) copolymers to improve the proton conductivity and control water absorption for membranes. The water absorption of **SP-*x*** membranes was investigated in detail (Table 2). Upon increasing the IEC of **SP-*x*** from 0.8 to 1.67 mEq g^{-1}, the water uptake increased from 4.3% to 30.5% at room temperature and from 7.0% to 46.8% at 80 °C, which indicates that all the membranes exhibit a lower water uptake than many random copolymers and single sulfonated side chain copolymers.[1,17] Additionally, **SP-*x*** membranes exhibited good dimension stability and the largest swelling ratio is lower than 24% at 80 °C, similar to that of Nafion 117. Fig. 6 shows the temperature effect on the water uptake and swelling ratios of **SP-*x*** copolymers. The water uptake and swelling ratio appear to exhibit similar trends, increasing as the temperature increases. Below 80 °C, both increased slowly. When the temperature went above 80 °C, the membranes with high amounts of sulfonated content exhibited a sharp increase in water sorption and swelling ratio, which is attributed to the formation of large and continuous ion networks in the sulfonated polymers.

The oxidative stabilities of the **SP-*x*** films were evaluated in Fenton's reagent at 80 °C for 1 h. Nafion 117, which is a typical proton exchange membrane, was used for comparison. The results are summarized in Table 2. For all membranes, no obvious weight loss was observed, and their properties such as flexibility and transparency were maintained after the test.

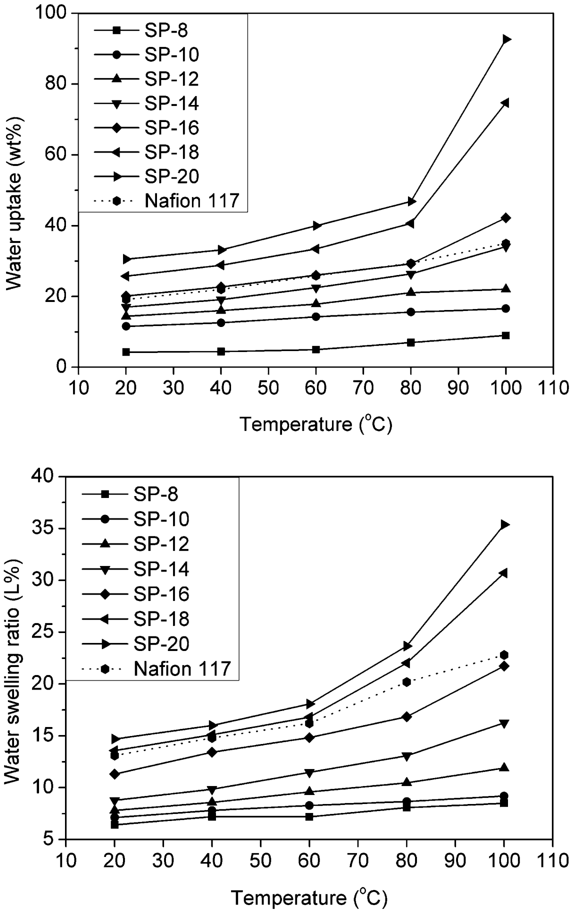

Fig. 6 Water uptake and swelling ratios of the **SP-*x*** and Nafion films as a function of temperature.

Proton conductivity

The proton conductivities of **SP-*x*** increased as the IEC values increased (listed in Table 3). Compared to Nafion membranes with similar IEC values, **SP-10** membranes exhibited slightly lower proton conductivities, however they were higher than those of many random copolymers. For example, the proton

Table 2 Some properties of sulfonated poly(arylene ether)s

Polymer	IEC (mEq g^{-1})	Water uptake (wt%)		Dimensional stability (L%)		Oxidative stability[a] (wt%)	Tensile strength[b] (MPa)	Elongation at break[b] (%)
		RT	80 °C	RT	80 °C			
SP-20	1.67	30.5	46.8	14.7	23.7	>99	39 (35)	16.9 (49)
SP-18	1.55	25.7	40.6	13.6	22.2	>99	41 (36)	13.4 (42)
SP-16	1.42	20.1	29.2	11.3	16.8	>99	43 (38)	12.5 (38)
SP-14	1.28	17.0	26.4	8.8	13.1	>99	46 (39)	10.4 (39)
SP-12	1.13	14.4	21.1	7.8	10.5	>99	46 (42)	9.7 (26)
SP-10	0.97	11.6	15.6	7.1	8.8	>99	48 (44)	9.4 (22)
SP-8	0.80	4.3	7.0	6.4	8.1	>99	51 (45)	8.2 (23)
Nafion 117	0.91	19.2	29.4	13.1	20.2	>97	38 (28)	205 (230)

[a] Residue weight after treatment in Fenton's reagent (3% H_2O_2 containing 2 ppm $FeSO_4$) at 80 °C for 1 h. [b] Measurements of dry membranes, values in parentheses represent properties of wet membranes.

Published on 12 November 2012. Downloaded by New York University on 08/10/2014 11:56:32.

Table 3 Proton conductivity and methanol permeability of the **SP-*x*** membranes

Polymer	IEC (mEq g^{-1})	σ (mS cm^{-1})		Methanol permeability (cm^2 s^{-1})	Methanol uptake^b (%)	Dimensional change^b (%)
		RT	80 °C			
SP-20	1.67	57	125	3.79×10^{-7}	59.7	18.7
SP-18	1.55	55	122	3.39×10^{-7}	53.4	19.6
SP-16	1.42	40	87	2.27×10^{-7}	39.8	15.0
SP-14	1.28	35	75	1.90×10^{-7}	40.9	16.2
SP-12	1.13	26	55	1.36×10^{-7}	24.4	7.3
SP-10	0.97	11	31	4.82×10^{-8}	13.5	5.1
SP-8	0.80	7	17	2.52×10^{-8}	15.6	5.4
SC-SPAE-100^a	1.81	—	75	3.28×10^{-7}	—	—
SC-SPAE-80^a	1.52	—	34	1.63×10^{-7}	—	—
Nafion 117	0.91	80	118	2.94×10^{-6}	—	—

^{a} Data from ref. 34. ^{b} Measured in 10 M methanol aqueous solution at 20 °C.

conductivities of SPAEK-6F-30 (IEC = 1.06 mEq g^{-1}) at room temperature and 80 °C are 4.5×10^{-3} S cm^{-1} and 1.1×10^{-2} S cm^{-1}, respectively,[34] which are much lower than those of **SP-10** (IEC = 0.97 mEq g^{-1}). Fig. 7 displays proton conductivities as a function of temperature. The proton conductivities of the **SP-*x*** membranes increased with increasing temperature. The highest proton conductivity of 162 mS cm^{-1} was observed for **SP-20** with an IEC of 1.67 mEq g^{-1} at 100 °C. In addition, the conductivities of **SP-20** and **SP-18** were higher than that of Nafion 117 under the same conditions. Compared to the SC-SPAE-X polymer (our previous work),[17] the **SP-*x*** exhibited higher proton conductivities (Table 3) at similar IEC levels. For example, the proton conductivity of **SP-18** (IEC = 1.55 mEq g^{-1}) is 122 mS cm^{-1}, which is much higher than that of SC-SPAE-80 (IEC = 1.52 mEq g^{-1}) which has a proton conductivity of 34 mS cm^{-1}. This is attributed to the high density sulfonic acid groups present in every side group, resulting in better hydrophilic–hydrophobic microphase separation morphology in the **SP-*x*** polymers.

Methanol permeability and selectivity

The **SP-*x*** copolymers exhibited lower methanol permeabilities than Nafion 117. The methanol permeability values for 10 mol L^{-1} methanol at room temperature were in the range 2.52×10^{-8} to 3.79×10^{-7} cm^2 s^{-1} which is several times lower than the value of 2.94×10^{-6} cm^2 s^{-1} for Nafion 117. The dimensional stabilities in high concentration methanol solution were also measured (Table 3), and slightly higher values than those in water were observed. In order to evaluate the combined effect of the proton conductivity and methanol crossover, a trade-off plot containing both methanol permeability and proton conductivity at room temperature is shown in Fig. 8. It is clear that the preferred membranes, which have higher proton conductivities and lower methanol permeabilities, are situated at the top right corner of the plot. The relationship between the methanol permeability, proton conductivity and IEC were investigated using a plot of selectivity *versus* IEC (Fig. 9). The selectivity, which is the ratio of the proton conductivity to the methanol permeability, is often used to evaluate the potential performance of DMFC membranes. It is a useful predictive parameter of performance, providing the proton conductivity is sufficiently high.[35] The selectivity of **SP-*x*** membranes decreased as the IEC value increased. In addition, the **SP-*x*** membranes displayed much higher selectivities than the Nafion membranes due to their low methanol permeabilities. The **SP-*x*** (IEC > 1.1 mEq g^{-1}) membranes exhibited high proton conductivities and

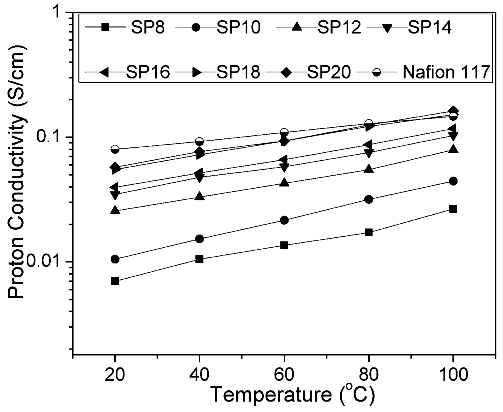

Fig. 7 Proton conductivity of **SP** films as a function of temperature.

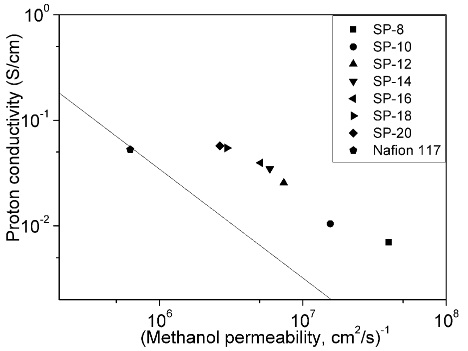

Fig. 8 Proton conductivity *versus* methanol permeability of the **SP-*x*** and Nafion 117 films at room temperature.

Published on 12 November 2012. Downloaded by New York University on 08/10/2014 11:56:32.

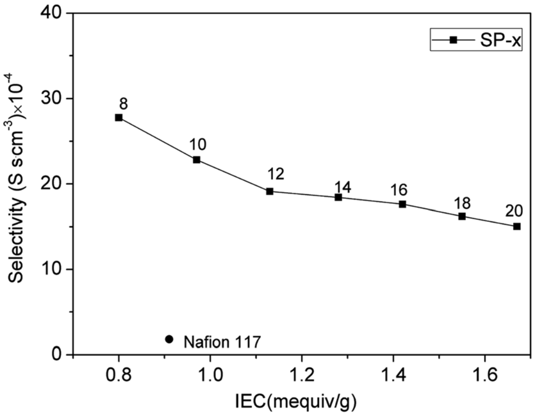

Fig. 9 Performance trade-off plot of IEC value *versus* selectivity.

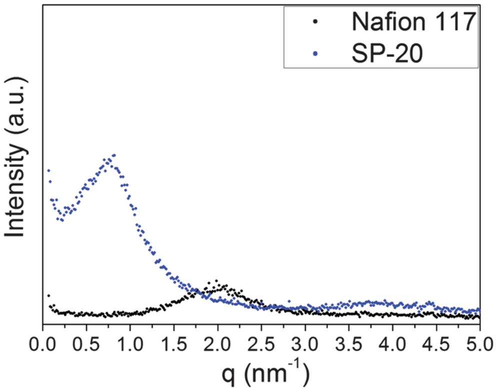

Fig. 10 The SAXS profiles of **SP-20** and Nafion 117.

low methanol permeabilities and could be promising materials for DMFC applications.

Mechanical properties

It is essential for PEMs to possess adequate mechanical strength under dry and humid conditions. Here, tensile tests of both dry and wet membranes were conducted at room temperature, and the results are summarized in Table 2. The strengths of the membranes of **SP-*x*** are higher than that of Nafion 117. These data indicate that these membranes are strong and tough.

Morphology

The morphological features of the completely amorphous ionomer membranes were studied by small-angle X-ray scattering (SAXS) measurements on membranes having the sulfonated domains selectively stained with Pb^{2+} to enhance the contrast.[36,37] In general, the extremely hydrophobic polymer backbones and the superacidity and hydrophilicity of the $-CF_2-SO_3H$ units in Nafion give rise to a distinct phase separation and a quite well-defined morphology. The hydrocarbon backbone is far less hydrophobic and the arylene sulfonic acid units far less acidic, which leads to a morphology with a less pronounced phase separation. The morphological differences between Nafion membranes and conventionally sulfonated hydrocarbon aromatic membranes have previously been extensively discussed by Kreuer and Jannasch on the basis of SAXS data.[15,37] As seen in Fig. 10, although the **SP-20** possessed a sulfonated poly(arylene ether) feature, the ionomer peak of the membrane was shifted towards a lower q-value ($q_{\max} = 0.75\ \mathrm{nm}^{-1}$), as compared to the profile of the Nafion 117 membrane ($q_{\max} = 2.00\ \mathrm{nm}^{-1}$). The values of $q_{\max}$ correspond to $d = 8.4$ and 3.14 nm, respectively, for the two ionomers. This result was attributed to a high local concentration of sulfonic acid groups, and their separation from the polymer main chain, which promoted a high degree of phase separation. Meanwhile a weak ionomer peak appeared at around 3.7 nm^{-1}, and this may be attributed to some sulfonic acid groups close to main chain with decreased mobility during the membrane formation.[38] As a consequence, a longer pendent group will be introduced into this series of polymer and further investigation is on going.

Conclusion

A novel difluoride monomer containing five electron-rich phenyl rings has been successfully synthesized. Based on this monomer, the poly(arylene ether sulfone) copolymer with a penta-sulfonic acid pendent was obtained by polycondensation, followed by sulfonation in high yields. ^{1}H NMR spectroscopy confirmed the structures of monomer and the corresponding copolymers. Tough, flexible and transparent sulfonated membranes (**SP-*x***) were obtained by a solution casting method, and showed excellent thermal stabilities and suitable mechanical properties. The hydrophilic microphase in the polymer significantly affected the proton transport, water absorption and dimensional stability. **SP-*x*** polymers with higher local concentrations of penta-sulfonic acid pendents exhibited lower water uptake, good dimensional stabilities and high proton conductivities. With low amounts of sulfonic acid groups (IEC = 0.92 mEq g^{-1}), **SP-10** exhibited a proton conductivity of $1.1 \times 10^{-2}\ \mathrm{S\ cm}^{-1}$ at room temperature. This performance was better than that of many sulfonated random polymers, and it achieved a standard of proton conductivity ($>10^{-2}\ \mathrm{S\ cm}^{-1}$) suitable for aromatic PEMs. **SP-20** (IEC = 1.67 mEq g^{-1}) exhibited similar properties to Nafion 117, including proton conductivity, water uptake and swelling ratio. Remarkably, the methanol permeability of **SP-20** was almost just one-tenth that of Nafion 117. All these features can be attributed to the special structure of **SP-*x*** copolymers, leading to good morphology in the polymer. The combination of good thermal stability, high proton conductivity, and low methanol permeability makes **SP-*x*** attractive as PEMs for fuel cell applications.

Acknowledgements

The authors would like to thank the China Natural Science Foundation (Grant no. 51103060) for financial support of this work.

Published on 12 November 2012. Downloaded by New York University on 08/10/2014 11:56:32.

References

1 M. A. Hickner, H. Ghassemi, Y. S. Kim, B. R. Einsla and J. E. McGrath, *Chem. Rev.*, 2004, **104**, 4587–4612.

2 H. Zhang and P. K. Shen, *Chem. Rev.*, 2012, **112**, 2780–2832.

3 A. K. Mishra, S. Bose, T. Kuila, N. H. Kim and J. H. Lee, *Prog. Polym. Sci.*, 2012, **37**, 842–869.

4 C. H. Park, C. H. Lee, M. D. Guiver and Y. M. Lee, *Prog. Polym. Sci.*, 2011, **36**, 1443–1498.

5 S. Bose, T. Kuila, T. X. H. Nguyen, N. H. Kim, K. Lau and J. H. Lee, *Prog. Polym. Sci.*, 2011, **36**, 813–843.

6 G. Alberti, M. Casciola, L. Massinelli and B. Bauer, *J. Membr. Sci.*, 2001, **185**, 73–81.

7 S. Kaliaguine, S. D. Mikhailenko, K. Wang, P. Xing, G. P. Robertson and M. D. Guiver, *Catal. Today*, 2003, **82**, 213–222.

8 J. Kerres, A. Ullrich, F. Meier and T. Haring, *Solid State Ionics*, 1999, **125**, 243–249.

9 G. Ye, N. Janzen and G. R. Goward, *Macromolecules*, 2006, **39**, 3283–3290.

10 X. Guo, J. Fang, T. Watari, K. Tanaka, H. Kita and K. Okamoto, *Macromolecules*, 2002, **35**, 6707–6713.

11 K. Miyatake, H. Zhou, H. Uchida and M. Watanabe, *Chem. Commun.*, 2003, 368.

12 K. Miyatake, H. Zhou and M. Watanabe, *Macromolecules*, 2004, **37**, 4956–4960.

13 D. J. Jones and J. Rozière, *J. Membr. Sci.*, 2001, **185**, 41–58.

14 R. Nolte, K. Ledjeff, M. Bauer and R. Müelhaupt, *J. Membr. Sci.*, 1993, **83**, 211–220.

15 K. D. Kreuer, *J. Membr. Sci.*, 2001, **185**, 29–39.

16 K. D. Kreuer, S. J. Paddison, E. Spohr and M. Schuster, *Chem. Rev.*, 2004, **104**, 4637–4678.

17 J. Pang, H. Zhang, X. Li and Z. Jiang, *Macromolecules*, 2007, **40**, 9435–9442.

18 Y. Chen, R. L. Guo, C. H. Lee, M. Lee and J. E. McGrath, *Int. J. Hydrogen Energy*, 2011, **37**, 6132–6136.

19 O. Celebi, C. H. Lee, Y. Lin, J. E. McGrath and J. S. Riffle, *Polymer*, 2011, **52**, 4718–4726.

20 X. Li, F. Paoloni, E. A. Weiber, Z. Jiang and P. Jannasch, *Macromolecules*, 2012, **45**, 1447–1459.

21 D. S. Kim, G. P. Robertson and M. D. Guiver, *Macromolecules*, 2008, **41**, 2126–2134.

22 J. Pang, H. Zhang, X. Li, B. Liu and Z. Jiang, *J. Power Sources*, 2008, **184**, 1–8.

23 J. Pang, H. Zhang, X. Li, L. Wang and Z. Jiang, *J. Membr. Sci.*, 2008, **318**, 271–279.

24 J. Pang, H. Zhang, X. Li, D. Ren and Z. Jiang, *Macromol. Rapid Commun.*, 2007, **28**, 2332–2338.

25 M. L. Einsla, Y. S. Kim, M. Hawley, H. S. Lee, J. E. McGrath, B. Liu, M. D. Guiver and B. S. Pivovar, *Chem. Mater.*, 2008, **20**, 5636–5642.

26 T. Higashihara, K. Matsumoto and M. Ueda, *Polymer*, 2009, **50**, 5341–5357.

27 K. Matsumoto, T. Higashihara and M. Ueda, *Macromolecules*, 2009, **42**, 1161–1166.

28 S. Matsumura, A. R. Hlil, C. Lepiller, J. Gaudet, D. Guay and A. S. Hay, *Macromolecules*, 2008, **41**, 277–280.

29 S. Matsumura, A. R. Hlil, C. Lepiller, J. Gaudet, D. Guay, Z. Shi, S. Holdcroft and A. S. Hay, *Macromolecules*, 2008, **41**, 281–284.

30 K. Sonogashira, Y. Tohda and N. Hagihara, *Tetrahedron lett.*, 1975, **50**, 4467–4470.

31 L. F. Fieser, *Org. Synth.*, 1973, **5**, 604.

32 B. Jung, B. Kim and J. M. Yang, *J. Membr. Sci.*, 2004, **245**, 61–69.

33 B. Liu, G. P. Robertson, D. S. Kim, M. D. Guiver, W. Hu and Z. Jiang, *Macromolecules*, 2007, **40**, 1934–1944.

34 P. Xing, G. P. Robertson, M. D. Guiver, D. S. Mikhailenko and S. Kaliaguine, *Macromolecules*, 2004, **37**, 7960–7967.

35 N. Li, D. S. Hwang, S. Y. Lee, Y. Liu, Y. M. Lee and M. D. Guiver, *Macromolecules*, 2011, **44**, 4901–4910.

36 N. Li, C. Wang, S. Y. Lee, C. H. Park, Y. M. Lee and M. D. Guiver, *Angew. Chem.*, 2011, **123**, 9324–9327.

37 B. Lafitte and P. Jannasch, *Adv. Funct. Mater.*, 2007, **17**, 2823–2834.

38 E. P. Jutemar and P. Jannasch, *J. Membr. Sci.*, 2010, **1–2**, 87–95.

This journal is © The Royal Society of Chemistry 2013